Infrared photodecomposition of $Fe(CO)_5$ using a TEA CO_2 laser

Tetsuro Majima

The Institute of Physical and Chemical Research (RIKEN), Hirosawa 2-1, Wako, Saitama 351-01 (Japan)

ABSTRACT AND CONTENTS

The 5 μm transient absorptions over the range 1910-2080 cm^{-1} and absorption energy were measured in the SF_6-sensitized infrared photodecomposition of $Fe(CO)_5$ using a transversely excited atmospheric (TEA) CO_2 laser. The rate-determining step is the first decarbonylation step ($Fe(CO)_5 \rightarrow Fe(CO)_4 + CO$), and the subsequent decarbonylation processes proceed in the stepwise manner and much faster than the first step. It is suggested that the formation of γ-iron ultrafine particles can be attributed to a high local temperature sufficient for the formation of γ-iron and rapid cooling because of the small particle size and using a short laser pulse.

A. INTRODUCTION

Most of the previous studies on the unsubstituted transition metal carbonyls, $M(CO)_n$, were carried out by UV light excitation to electronically excited states [1]. In contrast, infrared multiple-photon decomposition (IRMPD) of $M(CO)_n$ was studied using a frequency-doubled TEA CO_2 laser [2] and an infrared p-H_2 Raman laser [3]. The strong 5 μm C-O stretching bands and 16-17 μm M-C-O bending vibrations of $M(CO)_n$ were excited. The primary process was interpreted to be scission of a single M-CO bond, followed by sequential decarbonylations, in both the UV-photolysis and IRMPD experiments.

Since $M(CO)_n$ does not absorb or absorbs only weakly in the tunable range (9-11 μm) of a TEA CO_2 laser, it is necessary to add an infrared photosensitizer when using a TEA CO_2 laser. Ideally, this should be a substance which absorbs infrared radiation strongly and transfers a sufficient portion of the absorbed energy to $M(CO)_n$ but does not decompose itself or participate in the reaction sequence. It has been well characterized that SF_6 absorbs strongly in the tunable range of a TEA CO_2 laser but does not decompose at a low laser fluence (ca. 2 J cm^{-2}) because of the relatively high threshold fluence for IRMPD. Indeed, the SF_6-sensitized pyrolysis of $Fe(CO)_5$ has been studied using CW and TEA CO_2 lasers [4,5].

We have found that $Fe(CO)_5$ decomposes efficiently into iron particles and CO by the SF_6-sensitized infrared photoreaction of a mixture of SF_6-$Fe(CO)_5$ using a TEA CO_2 laser [6]. A part of experimental results has been

0010-8545/94/$26.00
SSDI 0010-8545 (94) 02016–C

reported previously: decomposition stoichiometry, trapping of the intermediates by PF_3, effects of additives, products analysis, time-resolved infrared absorption measurements, and absorption energy measurements [6-8]. One remarkable finding was the formation of ultrafine particles of γ-iron with a face-centered-cubic (fcc) structure, which is usually stable at 1183-1662 K and therefore can not normally be isolated at room temperature. In this paper we wish to report the SF_6-sensitized infrared photodecomposition of $Fe(CO)_5$ mainly on the basis of time-resolved infrared transient absorption measurements and absorption energy measurements.

B. STOICHIOMETRY AND TRAPPING OF THE INTERMEDIATES

Upon irradiation of a mixture of SF_6 (1 Torr, 133.322 Pa) and $Fe(CO)_5$ (1 Torr) with an unfocused laser beam of ca. 0.1-0.15 J cm^{-2} incident laser fluence at 940.55 cm^{-1} tuned to the SF_6 ν_3 band, the decomposition of $Fe(CO)_5$ efficiently occurred via SF_6-photosensitized process. Only CO was obtained as a volatile product, while fcc γ-iron ultrafine particles were formed in place of α-iron with a body-centered-cubic (bcc) structure. No other products were detected by any analyses. On the other hand, SF_6 was recovered with a 100% yield. The ratio of yield of CO to the consumption of $Fe(CO)_5$ was measured to be ca. 5 at each laser shot. Therefore, the stoichiometry of the decomposition is $Fe(CO)_5 \rightarrow Fe + 5\,CO$, for each laser shot.

When a mixture of SF_6 (0.5 Torr) and $Fe(CO)_5$ (0.2 Torr) was irradiated in the presence of excess PF_3 (10 Torr), $Fe(CO)_4(PF_3)$ was detected as a dominant product at lower conversion. Therefore, the initial decomposition reaction is the dissociation of one CO from $Fe(CO)_5$, and the further decarbonylations from $Fe(CO)_4$ proceed sequentially until Fe atom, similarly to the results from UV-photolysis [1] and IRMPD of $Fe(CO)_5$ [2,3].

C. 5 μm TRANSIENT ABSORPTION MEASUREMENTS

We applied 5 μm transient absorption measurements to study the kinetics of the SF_6-sensitized infrared photodecomposition of $Fe(CO)_5$ using a TEA CO_2 laser. The time-resolved infrared spectrometer used in this study has been described previously [8]. The experimental setup is illustrated in Fig. 1. A Lumonics 821 TEA CO_2 laser was set to the 10P(24) line at 940.55 cm^{-1}, which is absorption peak of SF_6 at high laser fluence. The probe beam from a tunable diode laser was sent in the opposite direction to the CO_2 laser beam through the reaction cell. An almost collinear arrangement was used, such that the narrow probe beam passed through the central part of the irradiated volume. Transient absorption signals were monitored by an HgCdTe detector, which had an overall response time of ca. 1 μs. The signals were based on a single shot measurement.

A mixture of 1.0 Torr SF_6 and 1.0 Torr $Fe(CO)_5$ was irradiated with a laser fluence of 0.15 J cm^{-2}. The time-resolved infrared absorption of CO, and vibrationally excited $Fe(CO)_5$, and the depletion of the absorption of $Fe(CO)_5$

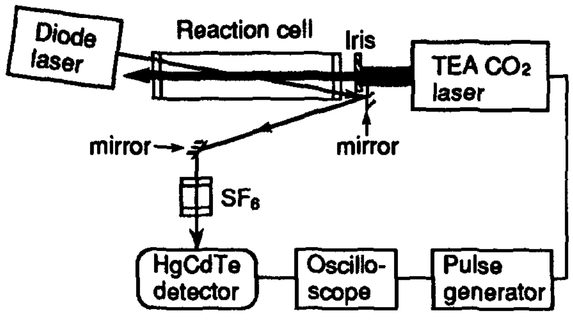

Fig. 1 Schematic diagram of the experimental arrangement for the 5 μm transient absorption measurements.

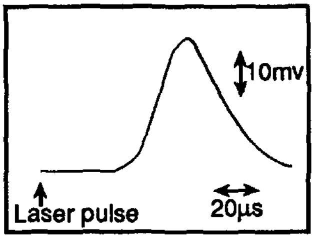

Fig. 2 Transient absorption by $Fe(CO)_2$ at 1920 cm^{-1}. An SF_6-$Fe(CO)_5$ (1:1) mixture of 2 Torr was irradiated with an incident laser fluence of 0.15 J cm^{-2}.

ν_6 and ν_{10} bands were measured over the range of 1975-2080 cm^{-1} using a tunable diode laser [8]. On the basis of the observed results and kinetic analyses, we summarize the results as follows: 1) the formation of CO (υ= 0) in the first decarbonylation step occurs with rate constant of $8.5x10^{-14}$ cm^3 $molecule^{-1}$ s^{-1} or grater (rise time of 364 μs Torr or less), 2) more than 95% of the dissociated CO is formed in the vibrational ground state, and 3) the depletion of vibrationally cold $Fe(CO)_5$ occurs with rate constant of $4.7x10^{-13}$ cm^3 $molecule^{-1}$ s^{-1} (rise time of 64 μs Torr), and 4) infrared absorption of vibrationally hot $Fe(CO)_5$, observed at 1977-2003 cm^{-1} region, shows fast rise time of the order of 5.4 μs Torr (rate constant of $5.7x10^{-12}$ cm^3 $molecule^{-1}$ s^{-1}). The formation of CO in the first decarbonylation step occurs much slower than the depletion of $Fe(CO)_5$ and the formation of vibrationally hot $Fe(CO)_5$. Therefore, the depletion of $Fe(CO)_5$ and the formation of vibrationally hot $Fe(CO)_5$ correspond to vibrational-translational/rotational (V-T/R) and vibrational-vibrational (V-V) energy transfers between SF_6 and $Fe(CO)_5$. The slow formation of CO in the first decarbonylation process indicates that the decomposition occurs thermally inspite of the fast V-V and V-T/R processes.

In order to elucidate the kinetics involving the coordinatively unsaturated species formed as the intermediate, we studied the time-resolved infrared absorption measurements over the range of 1905-1940 cm^{-1}. No infrared absorption of vibrationally hot $Fe(CO)_5$ was observed, while the transient absorption was observed in the range of 1910-1930 cm^{-1} as shown in Fig. 2. The absorption had an induction period of about 90 μs Torr after the laser pulse, grew in a time scale of 40 μs Torr, and decayed in a time scale of 60 μs Torr. The wavenumber of the absorption is nearly same to that of $Fe(CO)_2$ formed in the UV-photolysis of $Fe(CO)_5$. Therefore, the absorption is reasonably assigned to $Fe(CO)_2$.

The total time for the transient behavior is ca. 200-250 μs Torr, corresponding to the formation and the decay of $Fe(CO)_2$. From the formation of $Fe(CO)_2$, the decarbonylation of $Fe(CO)_3$ into $Fe(CO)_2$ plus CO occurs in a time scale of 40 μs Torr. From the decay of $Fe(CO)_2$, the decarbonylation of $Fe(CO)_2$ into Fe(CO) plus CO occurs in a time scale of 60 μs Torr. On the other hand, CO formation in the first decarbonylation step has a rise time of 364 μs Torr or less, which is much slower than the subsequent decarbonylation processes. Therefore, it is suggested that the rate-determining step is the first step, and the subsequent decarbonylation processes occur in the stepwise manner and proceed much faster than the first one under the condition.

The induction period of about 90 μs Torr can not be directly compared with the rise time of 364 μs Torr or less for the first decarbonylation step, estimated by kinetic analyses according to stepwise and sequential decarbonylations. However, the induction period must be related to the time for reaction processes before generation of $Fe(CO)_2$. In other words, the decarbonylation steps of $Fe(CO)_5$ into $Fe(CO)_3$ proceed in a time scale of 90 μs Torr. Therefore, it is strongly suggested that the decarbonylations occur after thermal equilibrium is attained via V-V and V-T/R processes, and the decarbonylations proceed in the stepwise manner, and that the first decarbonylation step is the rate-determining one.

D. DECOMPOSITION MECHANISM

On the basis of the observed results, the following decomposition mechanism is suggested (Scheme 1): infrared multiple-photon absorption (IRMPA) of SF_6 via ν_3 mode to yield a vibrationally excited $SF_6^{\ddagger}$ (the dagger denotes vibrational excitation) (eq. 1). The V-V transfer from $SF_6^{\ddagger}$ to $Fe(CO)_5$ occurs very rapidly, with a rate constant of 5.7×10^{-12} cm^3 $molecule^{-1}$ s^{-1}, to form $Fe(CO)_5^{\ddagger}$ (eq. 2). Decarbonylation does not proceed directly from $Fe(CO)_5^{\ddagger}$. It is suggested that $Fe(CO)_5^{\ddagger}$ does not have enough internal energy for dissociation of one CO, and that $Fe(CO)_5^{\ddagger}$ needs to be excited higher via further V-V processes between $Fe(CO)_5^{\ddagger}$ and $SF_6^{\ddagger}$ or $Fe(CO)_5^{\ddagger}$ and via collisional V-T/R processes between $Fe(CO)_5^{\ddagger}$ and SF_6 or $Fe(CO)_5$ (eq. 3). In other words, thermal equilibrium is attained with a rate constant of 4.7×10^{-13} cm^3 $molecule^{-1}$ s^{-1} before decarbonylation. Thus the energy absorbed via IRMPA of SF_6 is converted into an internal energy of $Fe(CO)_5{}^*$ (the asterisk denotes thermal excitation). When $Fe(CO)_5{}^*$ has an internal energy higher than the dissociation threshold, the rate-determining decarbonylation of $Fe(CO)_5{}^*$ into $Fe(CO)_4$ and CO occurs with a rate constant of 8.5×10^{-14} cm^3 $molecule^{-1}$ s^{-1}, in which CO is formed only in the vibrational ground state (eq. 4). The coordinatively unsaturated $Fe(CO)_4$ regenerates $Fe(CO)_5$ via a back reaction with CO (eq. 5), or decomposes sequentially into $Fe(CO)_3$, $Fe(CO)_2$, Fe(CO), Fe and CO through thermal processes (eqs. 6-8). Finally a nucleation process of iron atoms occurs to yield ultrafine particles of metallic iron (eq. 9), while CO is the gaseous final product. The decomposition is quenched by temperature cooling via thermal conduction to the gas mixture in the nonirradiated volume. Since dissociation of one Fe-CO bond in $Fe(CO)_5$ is the rate-determining step, the sequential decarbonylations occur thermally once $Fe(CO)_4$ is formed until the gas mixture cools by thermal conduction and diffusion.

$SF_6 + nh\nu \rightarrow SF_6^{\ddagger}$ (1)
$SF_6^{\ddagger} + Fe(CO)_5 \rightarrow SF_6^{\ddagger} + Fe(CO)_5^{\ddagger}$ (2)
$Fe(CO)_5^{\ddagger} + R \rightarrow Fe(CO)_5^{*} + R^{*}$ (3)
$Fe(CO)_5^{*} \rightarrow Fe(CO)_4 + CO\ (\upsilon = 0)$ (4)
$Fe(CO)_4 + CO \rightarrow Fe(CO)_5$ (5)
$Fe(CO)_{4-m} + R^{*} \rightarrow Fe(CO)_{4-m}^{*} + R$ (6)
$Fe(CO)_{4-m}^{*} \rightarrow Fe(CO)_{3-m} + CO$ (7)
$Fe(CO)_{3-m} + CO \rightarrow Fe(CO)_{4-m}$ (8)
Fe→ γ-iron ultrafine particles (9)

Scheme 1. The reaction mechanism. $R \equiv SF_6, Fe(CO)_5$; $m = 0, 1, 2$ and 3; ‡ and * denote vibrational and thermal excitation respectively.

E. ABSORPTION ENERGY AND TEMPERATURE

We measured the energy absorbed by the gas mixture using a beam splitter placed in front of the entrance window of the cell and two pyroelectric power meters to monitor both the incident and the transmitted energies, and also using a microphone placed inside the cell to detect photoacoustic signals [8]. The average number of photons absorbed per SF_6 molecule $<n>$ can be obtained from the absorbed energy and the number of SF_6 molecules in the irradiated volume as a function of the mean fluence $<F>$ along the cell. $<F>$ is calculated by assuming Beer's law over the cell length as $<F> = F(1-\exp(-\ln Z))/(-\ln Z)$, where F is the incident laser fluence and Z is the transmittance. We obtained a linear relation between $\ln<n>$ and $\ln<F>$ for the SF_6-$Fe(CO)_5$ mixture, *i.e.* $<n>$ is proportional to $<F>^{0.80\pm0.02}$ under the following conditions: SF_6-$Fe(CO)_5$ (1:1) mixture at a total pressure of 2.0 Torr.

The temperature (T) in the irradiated volume was calculated from $<n>$, assuming that all the absorbed energy was thermalized and that T was homogeneous in the irradiated volume. For example, T is 610 K for a mixture of SF_6 (1.0 Torr) and $Fe(CO)_5$ (1.0 Torr) at $<n> = 5$ and $F = 0.15$ J cm^{-2}.

F. FORMATION OF γ-IRON ULTRAFINE PARTICLES

According to the simple thermal mechanism, T is estimated to be 610 K under our standard experimental conditions and not enough high to form of ultrafine particles of γ-iron, which are usually stable at 1183-1662 K. This can probably be attributed to an inhomogeneous temperature distribution in the cell as well as in the pump laser beam. Since the sample is optically thick, the temperature of molecules is not homogeneous in the irradiated volume and decrease along the beam axis. In fact, the temperature difference between entrance and exit in the cell is expected to be 50-100 K under our standard experimental conditions. The energy distribution of the multimode

TEA CO_2 laser beam is essentially inhomogeneous for each point. In addition, beam propagation for a long distance was about 5 m in the experimental arrangement. Therefore the energy distribution changes to a highly inhomogeneous profile in the cell. Therefore, the non-linear nature of IRMPA leads to a high local temperature which is sufficient for the formation of ultrafine particles of γ-iron, at least in the initial stage of $Fe(CO)_5$ decomposition before thermalization of all gaseous species.

When the reaction temperature reached to be 1183-1662 K, γ-iron is predominantly formed via nucleation and crystallization processes in place of α-iron. In the case of bulk iron, fcc γ-phase is stable only at 1183-1662 K, but transforms to the stable bcc α-phase on cooling to room temperature. However, the γ-iron ultrafine particles formed in the present reaction cool down without transforming to α-iron. This is probably attributable to rapid cooling because of the relatively small particle size (7.6 nm of mean particle size) of γ-iron particles, and the time scale of heating and cooling using a short pulse with duration of 100 ns plus 1.3 μs tail from a TEA CO_2 laser. The time scale is expected to be 0.1-few hundreds μs in the present experimental conditions.

The author is indebted to Dr. Michio Takami (RIKEN) for his collaboration, Dr. Yoshiyasu Matsumoto (The Institute of Molecular Science) for time-resolved infrared absorption measurements, Dr. Tessyu Miyahara (Dainippon Ink Co.) for magnetic measurements, Prof. Koichi Haneda (Ishinomaki Senshuu University) for Mössbauer spectroscopy, and Prof. Tadahiro Ishii (Science University of Tokyo) for product analysis. The author would like to thank Dr. J. P. Lillis (RIKEN) for reading the original manuscript and suggesting revisions in its English.

G. REFERENCES

1 J.T. Yardley, G. Gitlin, G. Nathanson and A.M. Rosan, J. Chem. Phys., 74 (1981) 370; I.M. Waller and J.W. Hepburn, ibid., 88 (1988) 6658.

2 M.-K. Au, P.A. Hackett, M. Humphries and P. John, Appl. Phys., B33 (1984) 43.

3 T. Majima, H. Tashiro, K. Midorikawa and M. Takami, Chem. Phys. Lett., 121 (1985) 65.

4 N.J. Bristow, B.D. Moore, M. Poliakoff, G.J. Ryott and J.J. Turner, J. Organomet. Chem., 260 (1984) 181.

5 G.P. Smith and R.M. Laine, J. Phys. Chem., 85 (1981) 1620; K.E. Lewis, D.M. Golden and G.P. Smith, J. Am. Chem. Soc., 106 (1984) 3905.

6 T. Majima, T. Ishii, Y. Matsumoto and M. Takami, J. Am. Chem. Soc., 111 (1989) 2417.

7 K. Haneda, Z.X. Zhou, A.H. Morrish, T. Majima and T. Miyahara, Phys. Rev. B, 46 (1992) 13832.

8 T. Majima, Y. Matsumoto and M. Takami, J. Photochem. Photobiol. A, 71 (1993) 213.